SmogStop™ Barrier Field Study

Report — Final Results

A Project Partnering Envision SQ Inc. and the University of Guelph, School of Engineering

Upon Request For Envision SQ Inc.
Completion Date: September 20, 2018
Prepared By: David Wood, E.I.T., Ph.D. & Bill Van Heyst, P.Eng., Ph.D.
Acknowledgments: Ministry of Transportation Ontario

CONTENTS

EXECUTIVE SUMMARY

Vehicle related air pollution currently poses a risk to public health and the environment. Photocatalysis has been shown to be an effective method to decompose nitrogen oxides (NO_x: NO and NO_2). The majority of research has focused on the use of titanium dioxide (TiO_2) for pollutant removal. However, a new patented photocatalyst, the SmogStop™, has been shown to more efficiently use the solar spectrum and does not have harmful byproducts. The photocatalytic reduction of NO_x will produce nitrogen gas (N_2) and oxygen gas (O_2), which are environmentally benign products.

Highway sound barriers are currently designed to protect residents from the noise created by highway traffic. The SmogStop™ barrier presents a novel method of removing traffic related air pollution while also protecting nearby residents from highway noise. Construction of the SmogStop™ barrier was completed in March 2017 at the intersection of Highway 401 and Bayview Avenue in Toronto, ON, on the north side of the highway. Since construction, the barrier has endured weathering from seasonal changes including: rain, wind, ice, snow, dust, road salt, etc. Data collection began August 18th, 2017 and continued until February 28th, 2018.

An environmentally controlled enclosed trailer was situated on site and was used to house all data logging equipment and gas analyzers. Integrated sampling heads were installed at the inlet and the outlet of the barrier to measure treated and untreated air. The relative difference between the two points was used to calculate the percent reduction. A 2-D sonic anemometer was installed in the middle of one of the bays to measure the velocity of the air moving through the barrier. This information was used for the determination of the volumetric flow rate and to develop a mass removal rate.

Atmospheric wind speed and direction as well as weather conditions for the area were obtained from the Toronto Pearson International Airport weather station (CYYZ) located approximately 25 km west of the study site.

There were two significant events that occurred during the study that were considered impactful in terms of the final results. The first was the resurfacing of the asphalt on the highway immediately in front of the field site which occurred on Sept 17th, 2017. The second was the closure of an open portion of the noise barrier beside the site location on December 21st, 2017. It is due to these events that performance calculations are considered to be conservative over the course of the field study. Performance measures presented herein are from August 18th, 2017 to February 28th, 2018.

The overall average reduction of NO_X was calculated to be 49% with the highest monthly average reduction occurring in February at 54%. The overall average was taken from the post-closure time period and conditions during this time are considered to be a more representative reflection of typical conditions for a barrier in service. The highest daytime and hourly reductions were determined to be 92% and 95%, respectively. Removal rates were also calculated on a mass basis (kilograms of NO_X removed/vehicle kilometer travelled/day). The average and maximum removal rates were calculated to be 0.88 and 13 kg/VKT/day during the daytime, respectively, which equated to 4100 and 61,000 VKT removed per day, respectively, from 1 km of road with the SmogStop™ barrier installed on one side. Reductions were also observed during the nighttime as a result of the high-mast lighting in the immediate vicinity of the barrier. Average removal rates during the nighttime were found to be 0.38 kg/VKT/day, which was equated to removing 1900 VKT per day, from 1 km of road with the SmogStop™ barrier installed on one side. The level of reduction at night may vary with the type of lighting system that is employed.

Introduction & Background

Vehicle related air pollution currently poses a risk to public health and the environment. Data from census block points and from the National Road Network indicates that nearly 32% of the Canadian population (approximately 10 million people) live in areas where they are exposed to traffic related air pollution (Brauer et al., 2012; Health Effects Institute, 2010). This includes those living 500 m from either side of a highway or 100 m from either side of a major urban roadway (Brauer et al., 2013). The transportation industry has been highlighted as a major contributor to atmospheric levels of nitrogen oxides (NO_X; including nitric oxide (NO) and nitrogen dioxide (NO_2)). In Canada, nearly 44% of NO_X emissions in 2015 were reportedly from the transportation industry alone (ECCC, 2017a).

In the atmosphere, NO quickly oxidizes into NO_2. In this form, NO_2 can dissolve in water vapor found in the atmosphere to form acids, which then react with other gases in the atmosphere to produce aerosolized nitrate particles known as secondary organic and inorganic aerosols (SOAs and SIAs). These particles contribute to the fine particulate matter size fraction ($PM_{2.5}$). Both NO_2 and its products from atmospheric reactions are harmful to humans and the environment. The primary adverse human health effect that stems from the inhalation of NO_2 is damage to the respiratory system. The negative health effects of NO_2 gas extend to animals and vegetative life as well. The acids formed when dissolved in water can damage buildings and materials, vegetation, cause the eutrophication of aquatic ecosystems, and direct damage to other organisms including animal life (ECCC, 2017b; Smith et al., 2009). In addition, NO_2, along with volatile organic compounds (VOCs) are the main pollutants responsible for the formation of ground level ozone, one of the primary components of smog. Smog is known to have harmful effects on humans and the environment (ECCC, 2017b; Xie et al., 2016; Bloomdahl et al., 2014; ECCC, 2013). Reducing the level of NO_X in the ambient air will help improve public health and mitigate the effects on the natural environment. A study in Toronto, Ontario, determined that there are 440 premature deaths and 1700 hospitalizations in the city annually that could be attributed to traffic related air pollution (McKeown, 2007). This study also demonstrated that the mortality related costs associated with traffic pollution were approximately $2.2 billion annually in Toronto. It was estimated that a 30% reduction in traffic related air pollution in Toronto alone could result

in 189 fewer deaths and $900 million less in health care costs per year. In Canada, it was estimated that nearly 21,000 premature deaths annually can be attributed to air pollution (CMA, 2008). On a global scale, the World Health Organization (WHO) estimates that approximately 7 million deaths were the result of air pollution in 2012 (WHO, 2014). In a report by the World Bank, the annual monetary cost from premature deaths due to air pollution was estimated to be over $5 trillion (World Bank, 2016).

Photocatalysts are emerging as a promising technology for the removal of a number of environmental contaminants. The majority of research has focused on the use of titanium dioxide (TiO_2) for pollutant removal, but the relatively large band gap energy (~3.2 eV) limits the use of this material to the UV spectrum (George et al., 2011). The SmogStop™ coating, a patented photocatalyst, makes efficient use of both the visible and the UV spectrum, making it better suited to applications within the solar spectrum. The photocatalytic removal of pollutants is achieved through photogenerated electron/hole pairs that reduce surface adsorbed species. The photocatalytic reduction of NO_X will produce nitrogen gas (N_2) and oxygen gas (O_2), which are environmentally benign products (Cheng et al., 2015).

Highway sound barriers are currently designed to protect residents from the noise created by highway traffic. The SmogStop™ barrier presents a novel method of removing traffic related air pollution while also protecting nearby residents from highway noise. This report summarizes the results from a field study using a 6.5 m tall SmogStop™ barrier (See Figure 1).

Field Study Timeline

The SmogStop™ barrier field installation was constructed near the intersection of Highway 401 and Bayview Avenue in Toronto, ON, on the north side of the highway. Construction was completed in March 2017. Since this time the installation has endured weathering from seasonal changes including: rain, wind, ice, snow, dust, road salt, etc.

Power was delivered to the site at the end of July 2017 and data collection began shortly thereafter, on August 18th, 2017 and continued until February 28th, 2018.

Important Dates

There were two significant events that occurred during the study that were considered impactful in terms of the final results. The first was the resurfacing of the asphalt on the highway immediately in front of the field site which occurred on Sept 17th, 2017. The second was the closure of an open portion of the noise barrier beside the site location on December 21st, 2017. As a result, data will be presented in four time frames, Pre-Road Work (August 18, 2017 – September 17, 2017), Post-Road Work (September 18, 2017 – December 21, 2017), Post-Closure (December 22, 2017 – February 28, 2018), and Full Study (August 18, 2017 – February 28, 2018).

Methodology

An environmentally controlled enclosed trailer was situated on site and was used to house all data logging equipment and two gas analyzers. The two Teledyne T200 chemiluminescent analyzers were used to measure NO_X concentrations. Calibrations were conducted using a 550 ppb NIST traceable calibration gas. As part of the NO_X sampling apparatus, custom designed sampling heads were used that spanned the entire 25 cm channel gap within the two walls of the SmogStop™ barrier to obtain a fully integrated transverse sample. The integrated sampling head pulled air through a 2 mm wide inlet at a flow rate of 50 l/min. The sampling head design as well as the high flow rate allowed for volumetric oversampling which the Teledyne analyzers then subsampled. The remainder of the sample was routed through an atmospheric dump to the outdoor environment. Two sampling points were used, one at the inlet of the barrier (top) and one at the outlet of the barrier (bottom) as shown in Figure 1 by arrows 1 and 2, respectively. The middle bay was coated with the SmogStop™ coating. It should be noted that the design of this sampling system allows for the removal rate to be determined for flow moving up or down in the channel. When air is moving up through the channel the bottom served as the inlet and the top as the outlet. The inlet sampling point was the untreated sample and the outlet served as the treated sample. The relative difference between the two points was used to calculate the percent reduction.

A 2-D sonic anemometer (Gill Instruments – WindSonic) was installed in the middle of bay 2 (to the right of the

coated bay) to measure the velocity of the air moving through the barrier, as shown in Figure 1 by arrow 3. This information was used for the determination of the volumetric flow rate and to develop a mass removal rate. Air flow through the 25 cm channel will be three dimensional in nature and can be subject to strong swirling motion dependent on the ambient wind direction and traffic conditions. Use of a 2-D anemometer will give a reasonable approximation of velocity through the channel, however, is subject to limitations given the 3-D nature of flow. In order to validate the measurements from the WindSonic, velocity profile measurements were performed manually using a TSI VelociCalc 9565 hotwire anemometer. Manual measurements were taken at the bottom of the barrier. Velocity profiles were developed across the 25 cm gap and velocity measurements were taken at the mid-point. Velocity profiles required 3 measurements (1 minute logging interval, 10 second time constant) at 23 locations across the 25 cm barrier gap. Measurements at the mid-point spanned a 2 hour duration. Measurements at the mid-point of the barrier gap were used to determine if the mid-point was an appropriate sampling location to represent the average velocity of the profile.

Atmospheric wind speed and direction as well as weather conditions for the area were obtained from the Toronto Pearson International Airport weather station (CYYZ) located approximately 25 km west of the study site.

All data for this field study was collected at 1 minute logging intervals using a 10 second time constant. All calculations referring to daytime and nighttime, within this report, accounted for the seasonally dependent time frames between sunrise and sunset.

Results & Discussion

Field Results

Figures 2-4 show the average wind velocity, average percent reduction, and average mass removal rate, respectively, for the entire study period as they relate to the atmospheric wind direction during the daytime. From Figure 2, it is evident that the highest wind velocities were from the West with South and North components. The largest average wind velocity was from the WSW, at 6.8 m/s. As illustrated in Figure 3, the highest average reduction of NO_x was 48% from the NNW. On a mass basis the largest reductions were recorded from the NNW and SW, as shown in Figure 4. The majority of the data

Figure 1: **Site photo showing the sampling locations (arrows 1 and 2) and 2-D anemometer location (arrow 3). Bays were numbered 1-5, moving from right to left.**

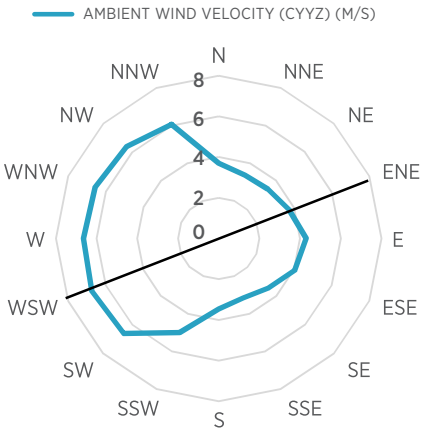

Figure 2: **Average wind velocity (m/s) as measured at Pearson International Airport (CYYZ) plotted as a function of direction (The black line indicates the orientation of the SmogStop™ barrier relative to north)**

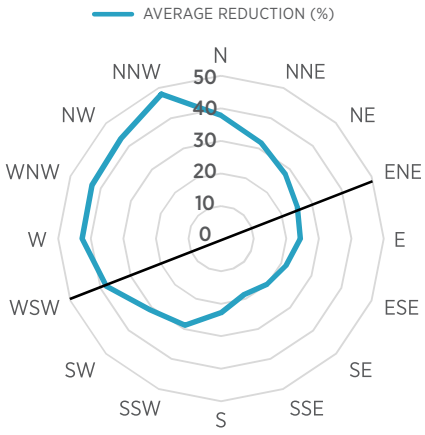

Figure 3: **Average percent (%) reduction in NO_x concentrations based on wind direction (The black line indicates the orientation of the SmogStop™ barrier relative to north)**

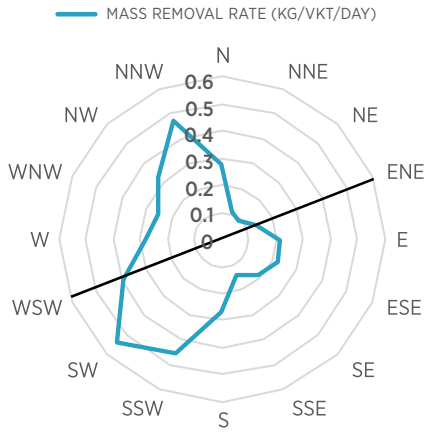

Figure 4: **Average mass removal rate (kg NO_x removed/VKT/day) of NO_x based on wind direction (The black line indicates the orientation of the SmogStop™ barrier relative to north)**

collected in this study had wind primarily from the North and the West. Therefore, it stands to reason that the largest reductions would be observed from these directions. In addition, the higher pressure zone on the highway side produced by the movement of traffic, allowed polluted air from the highway to flow down the SmogStop barrier channel, even when the dominant wind direction was from the backside of the barrier. This was confirmed through field observations and velocity measurements.

Average monthly reductions of NO_x are presented in Table 1, and average reductions are presented in Table 2 by time period. Tables 1 and 2 allow for the changes in efficiency to be observed in relation to the road work and noise barrier closure activities.

Table 1 indicates that the average daytime reductions from the month of August dropped in September, in connection to the asphalt resurfacing on September 17th. The reduced efficiency of the SmogStop® barrier was primarily due to the reduced photocatalyst surface area from airborne particulates, related to the paving operations, adhering to the coated surface. Scanning electron microscope (SEM) images were used to confirm the presence of the contaminant on the SmogStop™ coating as illustrated in the SEM images in Figures 5 and 6. Figure 6 shows the contaminant forming a film over the SmogStop™ material thus preventing any contaminated air from coming in contact with the photocatalyst. The covered surface area is believed to be a permanent loss in performance of the barrier and the primary factor in the decrease in efficiency. In future installations, restricting or closing the opening of the barrier on the highway side, during paving operations, will prevent any contamination from entering the channel and interfering with the photocatalyst.

As shown in Table 1, following the closure of the open section of noise barrier, on December 21st, a 2-fold increase in reductions were measured from December to January (from 26% to 51%, respectively). The higher level of reduction was also evident in February. The increase in reduction was likely the result of changing the flow dynamics in the vicinity of the SmogStop™ barrier. As shown in Figure 7, the unfinished section was close enough to the SmogStop™ barrier that closing it changed the air flow configuration. Air flow was no longer able to move around the barrier and through the unfinished section but was forced into the face of the barrier. This resulted in an increase in air flow over top of the SmogStop™ barrier which increased the amount of ground level pollution that traveled to the inlet.

Table 1: **Average monthly daytime reductions of NO_x**

Month	NO_x Reduction (%)
Aug (18th – 31st)	38%
Sept (full month)	22%
Nov (full month)	21%
Oct (full month)	25%
Dec (full month)	26%
Jan (full month)	51%
Feb (full month)	54%

Table 2: **Average daytime reductions presented by time period**

Event	Dates	NO_x Reduction (%)
Pre-Road Work	Aug 18, 2017 – Sept 16, 2017	30%
Post-Road Work	Sept 17, 2017 – Dec 21, 2017	23%
Post-Closure	Dec 22, 2017 – Feb 28, 2017	49%
Full Study	Aug 18, 2017 – Feb 28, 2018	34%

Table 3: **Average and maximum daytime and hourly reductions of NO_x**

	Daytime Reduction (%)	Hourly Reduction (%)
Average	34%	33%
Maximum	92%	95%

The changes in efficiency with time period are also evident in Table 2 with efficiencies of 30%, 23%, and 49%, during the Pre-Road Work, Post-Road Work, and Post-Closure time frames, respectively. The overall average reduction of NO_x for the full study was calculated to be 34%. Average and maximum daytime and hourly reductions for the full study are presented in Table 3.

WindSonic and Hot Wire Comparison

Figure 8 illustrates the comparison between the WindSonic measurements and the velocity profile that was developed across the 25 cm gap. During the time frame when these measurements were taken there was an ambient wind velocity of 3.2 m/s from a SSW direction. The average of the velocity profile was found to be 0.6 m/s and it can be seen that the measurement from the WindSonic during the same time frame was a close approximation of the profile average. All profile measurements also fall within one standard deviation (as shown by error bars) of the WindSonic average. This demonstrates that a large portion of the variability in the velocity measurements was captured by the WindSonic. Comparisons were made under a number of wind conditions and all show good agreement between the manual measurements and the WindSonic with the exception of instances when winds were out of the NW. When the ambient wind direction was from the NW the WindSonic underestimated the average flow as compared to the hot wire anemometer. Therefore, the WindSonic measurements are considered to be conservative when ambient winds are from the NW direction. The conservatism of this measurement is an important consideration given that a large

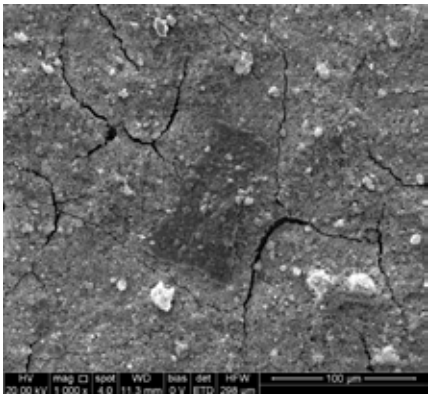

Figure 5: **SEM image of the SmogStop™ coating with a patch of the contaminant (darker rectangular patch in the center of the image) adhered to the coated surface at 1,000x magnification**

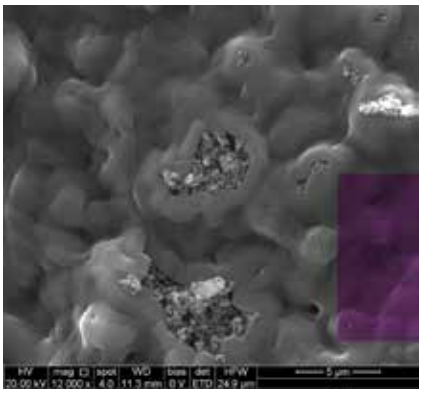

Figure 6: **Magnified SEM image from Figure 5 of the SmogStop™ coating with the contaminant adhered to coated surface at 12,000x magnification**

Figure 7: **3-D Google image of the field site identifying the SmogStop™ barrier location and the unfinished section (The image was taken prior to the construction of the new noise barrier, however, the opening remained in place due to underground infrastructure.)**

portion of the time in the fall and winter the dominant wind direction was from the NW.

Nighttime Reduction

Throughout the analysis of the field results, reductions during the nighttime were observed. This was the result of the high-mast lighting used to illuminate the highway during the evening hours. The high-mast lighting in this section of the highway used 12 x 1000 W high pressure sodium bulbs on each mast to keep the area well illuminated at night. As shown in Figure 9, a mast was situated in close proximity (~30 m) to the SmogStop™ barrier. High pressure sodium bulbs emit a significant amount of visible light and a small portion of UV-A, both of which have been shown to activate the SmogStop™ coating.

Table 4 summarizes the NO_x reduction efficiencies that were calculated for each of the four time periods of interest. The reductions were observed to follow a similar trend as the daytime reductions with respect to

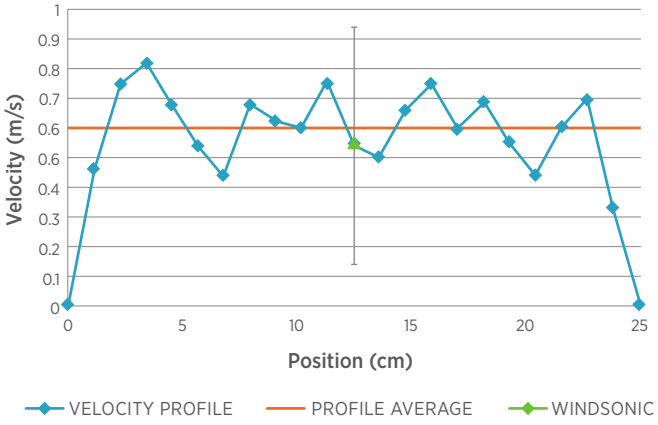

Figure 8: **Velocity profile and profile average as measured by hot wire anemometer and WindSonic measurement (± 1 Standard Deviation) during the same time frame.**

Figure 9: **Image from behind the SmogStop™ barrier showing the high-mast lighting nearby at night**

Table 4: **Average nighttime reductions presented by time period**

Event	Dates	NO_x Reduction (%)
Pre-Road Work	Aug 18, 2017 — Sep 16, 2017	29%
Post-Road Work	Sept 17, 2017 — Dec 21, 2017	22%
Post-Closure	Dec 22, 2017 — Feb 28, 2017	44%
Full Study	Aug 18, 2017 — Feb 28, 2018	32%

the road work and barrier closure activities. While on a percentage basis the reduction efficiencies appear to be similar in magnitude to the daytime reductions, on a mass basis differences were observed and are discussed in the following section.

Mass Removal Rate

Understanding the removal capacity of the SmogStop™ barrier in terms of the mass of NO_x removed is an important component of the analysis. Table 5, summarizes the maximum and average removal rates of the SmogStop™ barrier in kilograms of NO_x removed per vehicle kilometer travelled per day (kg NO_x Removed/VKT/day). The maximum removal rate was observed early on in the sampling campaign prior to the contamination from the road work. However, the two averages were calculated from the post-closure time period in order to demonstrate a more representative removal rate. Also, a scaling factor was applied to the velocity through the barrier in this calculation in order to account for the conservatism in the WindSonic measurement. Using a fleet-wide emission rate collected from the Motor Vehicle Emission Simulator (MOVES) for the 2016 vehicle fleet, an equivalent number of vehicles removed from a kilometer of road with the SmogStop™ barrier on one side was estimated. The assumptions used to generate the emission rate were a 30 year age distribution, average speed of 90 km/h, highway driving cycle, and a 60/40 split between passenger cars and light duty trucks (including SUVs and pickup trucks). The average nighttime removal rate was found to be roughly 43% of that of daytime, illustrating the diminished capacity for removal over the nighttime due to the change in lighting source.

Conclusions

The SmogStop™ barrier field study began August 18th, 2017 and was completed at the end of February 2018. Manual velocity measurements taken with a hotwire anemometer validated the use of the 2-D WindSonic anemometer to estimate the velocity of air moving through the channel. However, it was concluded that the WindSonic measurements were conservative when the ambient wind was from the NW direction.

The average monthly NO_x reduction of the barrier ranged from 21%-54%. The resurfacing operations and barrier closure activities that occurred during the field study had an impact on the overall efficiency of the system. The overall average daytime reduction efficiency of the barrier was found to be 34% over the entire duration of the study. Reductions were also observed during the nighttime due to the high-mast lighting in the area, calculated at an average reduction 32% over the duration of the study. Given that the two events that occurred during the study had impacts on the results, the calculations presented within this report are considered to be conservative. The daytime maximum and average mass removal rates of the barrier were calculated to be 13 and 0.88 kg of NO_x/VKT/day, respectively. These values equate to approximately 61,000 and 4100 VKT removed per day, respectively, from 1 km of road with the SmogStop™ barrier installed on one side. The average nighttime removal rate was calculated to be 0.38 kg of

Table 5: **Maximum and Average (Post-closure) SmogStop™ barrier removal rates in kilograms of NO_x removed and vehicles removed**

	kg NO_x Removed/VKT/day	VKT Removed/SmogStop™ km/day
Maximum Observed	13	61,000
Average (Daytime)	0.88	4100
Average (Nighttime)	0.38	1900

NO_X/VKT/day, representing roughly 43% of the daytime removal capacity. During the Post-Closure time period it was found that the overall average daytime reduction of NO_X was calculated to be 49% with the highest monthly reduction occurring in February, post-closure, at 54%. The highest daytime and hourly reductions were determined to be 92% and 95%, respectively.

References

Bloomdahl, R., Abualfaraj, N., Olson, M., & Gurian, P. L. 2014. Assessing worker exposure to inhaled volatile organic compounds from Marcellus Shale flowback pits. Journal of Natural Gas Science and Engineering 21: 348-356.

Brauer M, Reynolds C., Hystad P. 2012. Traffic-related air pollution and health: a Canadian perspective on scientific evidence and potential exposure-mitigation strategies. Vancouver (BC): University of British Columbia. Available: http://hdl .handle .net /2429/41542 (Accessed Sept 27/2017).

Brauer M, Reynolds C., Hystad P. 2013. Traffic related air pollution and health in Canada. Canadian Medical Association Journal. 185(18): 1557-1558. DOI: 10.1503

Canadian Medical Association (CMA). 2008. No breathing room: national illness costs of air pollution. Ottawa (ON): Canadian Medical Association. Available: www .cma.ca/ index.php/ci_id/86830/la_id/1.htm (accessed Oct 10, 2017).

Cheng, L., Zhu, M., Qiu, L., Payton, A., and Sakai, T. 2015. Report: Photocatalyst Testing for NO_X Decomposition. Impact Center, University of Toronto.

Environment and Climate Change Canada. 2013. Volatile Organic Compounds (VOCs). Government of Canada. Available: http://ec.gc.ca/air/default. asp?lang=En&n=15B9B65A-1 (Accessed: Sept 27/2017).

Environment and Climate Change Canada. 2017a. Nitrogen Oxide Emissions. Government of Canada. Available: https://www.ec.gc.ca/indicateurs-indicators/default. asp?lang=en&n=0870FFFC-1. (Accessed: Oct 10/2017)

Environment and Climate Change Canada. 2017b. Nitrogen Oxides - NO_X. Government of Canada. Available: https://www.ec.gc.ca/air/default. asp?lang=En&n=489FEE7D-1 (Accessed: Oct 10/2017).

George, S., Pokhrel, S., Ji, Z., Henderson, B. L., Xia, T., Li, L., & Mädler, L. 2011. Role of Fe doping in tuning the band gap of TiO_2 for the photo-oxidation-induced cytotoxicity paradigm. Journal of the American Chemical Society 133(29): 11270-11278.

Health Effects Institute. 2010. Traffic-related air pollution: a critical review of the literature on emissions, exposure, and health effects. Final Version of Special Report No. 17. Boston (MA). Available: http://pubs.healtheffects.org/ view.php?id=334 (Accessed Oct 10/2017).

McKeown, D. 2007. Toronto Public Health. Air pollution burden of illness from traffic in Toronto – Problems and Solutions. Toronto, Canada. Available: http:// www.toronto.ca/legdocs/mmis/2007/hl/bgrd/ backgroundfile-8046.pdf (Accessed Oct 10/2017).

Smith K.R., Jerrett M., Anderson H.R., Burnett R.T., Stone V., Derwent R., Atkinson R.W., Cohen A., Shonkoff S.B., Krewski D., Pope III C.A., Thun M.J., Thurston G. 2009. Public health benefits of strategies to reduce greenhouse-gas emissions: health implications of short-lived greenhouse pollutants. The Lancet 374(9707): 2091-210.

World Bank Group. 2016. The cost of air pollution: Strengthening the economic case for action. Available: http://documents.worldbank.org/curated/en/78152147317 7013155/pdf/108141-REVISED-Cost-of-PollutionWeb CORRECTEDfile.pdf (Accessed: Sept 27/2017).

WHO (World Health Organization). 2014. Burden of disease from the joint effects of Household and Ambient Air Pollution for 2012. Available: http://www. who.int/phe/health_topics/outdoorair/databases/ AP_jointeffect_BoD_results_March2014.pdf?ua=1. (Accessed: Sept 27/2017)

Xie, Y., Dai, H., Dong, H., Hanaoka, T., & Masui, T. 2016. Economic impacts from PM2. 5 pollution-related health effects in China: a provincial-level analysis. Environmental science & technology 50(9): 4836-4843.